JOURNAL OF Materials CHEMISTRY

Crystal chemistry of mixed Bi^{3+}–A^{n+} (A^{n+} = Na^+, K^+, Sr^{2+}, Ba^{2+}, Tl^+, Pb^{2+}) vanadium hollandite materials

Olivier Mentré,* Anne-Claire Dhaussy and Francis Abraham

Laboratoire de Cristallochimie et Physicochimie du Solide URA, CNRS 452, ENSCL , Université des Sciences et Technologies de Lille, BP 108, 59652 Villeneuve d'Ascq Cedex, France. E-mail: mentre@ensc-lille.fr

Received 7th December 1998, Accepted 21st January 1999

Hollandite oxides, $A_xBi_yV_8O_{16}$ (A = Na, K, Sr, Ba, Tl, Pb) with varying x, y ratios have been synthesized and studied. The feasibility of obtaining such materials under our normal solid state conditions is to be highlighted considering the fact that previous work on potassium-only compounds required high pressure and high temperature. It is therefore noteworthy that introduction of Bi^{3+} in the framework is easier than for A^{n+} co-cations. Crystal structures refined from single crystals of nominal compositions $A_{\approx 0.5}Bi_{\approx 1.1}V_8O_{16}$ evidenced a segregation between A^{n+} and Bi^{3+} ions. They respectively occupy the center of a square prism (K, Sr, Ba, Pb cases) and the center of a quasi-square plane (Bi^{3+}) while Na^+ and Tl^+ behave differently. This involves, since the tunnels are almost fully occupied, the impossibility of cohabitation of the same tunnels by the two antogonist species which would lead to an unrealistic A–Bi distance of 1.5 Å. The preparation of polycrystalline $ABiV_8O_{16}$ samples, in which the tunnels are filled, indicates a disordered distribution of A- and Bi-only tunnels since no supercell diffraction lines were observed. Finally electric conductivity measurements on mixed K–Bi materials are in agreement with a hopping semiconductivity due to the V^{3+}–V^{4+} mixed valence of the transition metal.

Introduction

A wide variety of compounds of formula $A_xM_8X_{16}$ crystallize with the hollandite-type crystal structure including oxides, hydroxides and sulfites.[1] Even FeOF oxyfluorite,[2] recently prepared in a supercritical fluid, crystallizes with that form rather than in the rutile crystal structure. Restricting our attention to the oxide class, the interest is evident because the simultaneous presence of two different oxidation states for the M transition metal predicts possible interesting electric properties. Furthermore, their tunnel structure is favourable for high ionic mobility as confirmed by the one-dimensional superionic conductivity behaviour of the $K_{2x}Mg_xTi_{8-x}O_{16}$.[3,4] Another proposed potential use is of a synthetic rock (SYNROC) containing hollandite as a major constituent, for use in the storage of radioactive wastes.[5] Vanadium is an interesting transition metal because of the high stability of the +3, +4 and +5 valences and so V-hollandite materials have been intensively studied.[6–10] In this connection, we recently evidenced and characterized $Bi_{1.7}V_8O_{16}$[11] which exhibits a mixed V^{3+}/V^{4+} valence and a semiconductor behavior. This oxide was the first example of Bi^{3+} introduction in the large 2×2 octahedra tunnels of the hollandite framework. It adopts the $I4/m$ space group of the ideal hollandite-type structure first described by Byström and Byström.[12] Its Pb^{2+} homologue of formula $Pb_{1.32}V_{8.35}O_{16.7}$[13] is strongly distorted and adopts a monoclinic symmetry, space group $I2/m$. Furthermore, $Bi_{1.7}V_8O_{16}$ was the basis of additional works stimulated by structural and electric/magnetic properties. Thus, Feldman and Müller–Buschbaum prepared $Bi_{1.7}Cu_4V_4O_{16}$[14] and also described the $Ba_{0.5}Bi_{0.9}V_8O_{16}$ crystal structure[15] included in our discussion. Finally, Ramakrishnan *et al.* measured the properties of $Bi_{1.7-x}Pb_xV_8O_{16}$[16] and Li-inserted compounds searching for possible superconductivity. The results were quite disappointing since no superconductivity, nor metallicity was encountered down to 12 K. A more structural approach encourages us to study the substitution of several cations for Bi^{3+} in $Bi_{1.7}V_8O_{16}$. Effectively, the Bi^{3+} coordination was found to be quasi-square planar, a novel and highly symmetric environment for this $6s^2$ lone pair cation. At the same time, most of the host cations are located at the center of a square prism within the tunnels, ≈1.5 Å distant from the bismuth site. Thus, mixed Bi^{3+}–A^{n+} hollandite compounds are good candidates for intertunnel ordering and X-ray detectable superstructure. Since both Bi^{3+} and A^{n+} can cohabitate in the same tunnel below a certain occupancy rate, it could at least lead to intratunnel cationic ordering. This work proposes the synthesis feasibility and the structural study of several $(A,Bi)_xV_8O_{16}$ oxides. For $A = K^+$ an electric investigation was carried out for several points of the solid solution while other cations such as $A = Na^+$, Ba^{2+}, Sr^{2+}, Pb^{2+} and Tl^+ led to a crystallographic-only characterization.

Experimental

Powder phases of $A_xBi_yV_8O_{16}$ were prepared by thermal treatment of the appropriate mixtures of AVO_3, for monovalent cations or $A_2V_2O_7$ for divalent cations and V_2O_5, V_2O_3 and Bi_2O_3. The mixtures were placed in a gold vessel introduced in a silica tube sealed under primary vacuum and annealed at 850 °C for 5 days. Intermediate $NaVO_3$, $TlVO_3$ and KVO_3 were previously prepared using the A^+ carbonate and V_2O_5 at 550, 350 and 400 °C, respectively. $Ba_2V_2O_7$, $Sr_2V_2O_7$ and $Pb_2V_2O_7$ were obtained by reaction between the A^{2+} carbonate and V_2O_5 at 700 °C in an alumina crucible. Our principal interest was the $ABiV_8O_{16}$ materials that should exhibit A/Bi cationic segregation for reasons explained below. The purity and crystallinity of the obtained materials were established using a Siemens D5000 diffractometer (Cu-Kα radiation) equipped with a graphite back monochromator yielding the unit cell parameters by least-squares refinement.

Single crystals were grown by reheating the powder of nominal $ABiV_8O_{16}$ compounds at 1200 °C in an evacuated quartz tube. Single crystals of mixed K–Bi, Sr–Bi, Pb–Bi, Tl–Bi hollandites were visually isolated and extracted from the melt while Na^+ and Ba^{2+} cations only developed crystals too small for conventional X-ray study. Therefore, we also report here results concerning the crystal structure of $Ba_{0.5}Bi_{0.9}V_8O_{16}$[15] study from Feldman and Müller–Buschbaum.

Table 1 Crystal data, intensity measurement and structure refinement parameters for $(A,Bi)_xV_8O_{16}$ materials

	$Sr_{0.5}Bi_{0.96}V_8O_{16}$	$Tl_{0.41}Bi_{1.24}V_8O_{16}$	$Pb_{0.4}Bi_{1.2}V_8O_{16}$	$K_{0.2}Bi_{1.45}V_8O_{16}$
Crystal data				
Formula weight	907.97	1006.46	997.19	974.38
a/Å	9.927(9)	9.986(13)	9.953(5)	9.944(3)
c/Å	2.898(3)	2.903(4)	2.900(2)	2.910(2)
V/Å^3	285.6(8)	289.5(8)	287.3(3)	287.7(3)
Data collection				
Standard reflections	$\bar{1}21$, $1\bar{2}1$, 130	$\bar{1}\bar{3}0$, $3\bar{1}0$, $1\bar{2}\bar{1}$,	$\bar{3}\bar{1}0$, $\bar{2}\bar{2}0$, $1\bar{3}0$	330, $31\bar{1}$, $\bar{1}2\bar{1}$
Number of measured reflections	1470	1502	1478	1486
Number of reflections $I>3\sigma(I)$	1027	690	648	863
Number of independent reflections	297	219	211	309
Limiting faces and distances (mm) from an arbitrary origin	001, $00\bar{1}$ 0.076 010, $0\bar{1}0$ 0.016 100, $\bar{1}00$ 0.011	001, $00\bar{1}$ 0.060 010, $0\bar{1}0$ 0.015 100, $\bar{1}00$ 0.010	001, $00\bar{1}$ 0.182 010, $0\bar{1}0$ 0.023 100, $\bar{1}00$ 0.023 $\bar{1}10$ 0.016	001, $00\bar{1}$ 0.090 010, $0\bar{1}0$ 0.019 100, $\bar{1}00$ 0.010
Linear absorption coefficient μ/cm^{-1}	230.46	301.12	297.42	276.97
Merging R factor R_{int} (%)	3.8	3.7	3.9	3.5
Refinement				
Number of refined parameters	26	25	28	28
$R=\sum[\|F_o\|-\|F_c\|]/\sum F_o$	0.047	0.044	0.041	0.029
$R_w=[\sum w(\|F_o\|-\|F_c\|)^2/\sum wF_o^2]^{1/2}$ with $w=1/\sigma(F_o)$	0.047	0.044	0.037	0.038

[a] Details in common: tetragonal, space group $I4/m$, $Z=1$, Phillips PW1100 diffractometer, λ(Mo-Kα) = 0.7107 Å (graphite monochromated) T = 198 K, w–2θ scan mode, scan width = 1.6°, θ range = 2–35°, recording reciprocal space: $-16\leqslant h\leqslant 16$, $-16\leqslant k\leqslant 16$, $0\leqslant l\leqslant 4$.

EDS (energy dispersive spectroscopy) microprobe elemental semiquantitative analysis was performed on a Philips 525 M scanning electron microscope connected to an EDAX PV 9900 analyser for potassium, strontium and thallium single crystals. It indicated the $K_{0.7}Bi_{1.3}$–$Sr_{0.4}Bi_1$– and $Tl_{0.5}Bi_{1.2}$–V_8O_{16} cationic distribution at least confirming the set of two different cations inside the V_8O_{16} framework. For all of the selected crystals, preliminary oscillation and Weissenberg photographs were consistent with the $I4/m$ space group. Neither diffuse superstructure spots nor diffuse streaks were observed.

Single crystal X-ray diffraction data were collected on a Philips PW 1100 automated four-circle diffractometer under the conditions given in Table 1. The intensity of each reflection was corrected for background and for Lorentz and polarization effects. Absorption corrections were performed using the analytical method of De Meulenaer and Tompa.[17]

Generally, the crystal structure refinement was performed in the $I4/m$ space group. After the introduction of the atomic coordinates extracted from the $Bi_{1.62}V_8O_{16}$ crystal structure, the Bi^{3+} occupancy was refined. Supplementary A^{n+} ions were located by the calculation of the subsequent Fourier difference synthesis. The occupancy was refined for Bi^{3+} and A^{n+} host cations. In the last cycles of refinement anisotropic displacements were considered at least for metallic atoms, leading to the final reliability factors presented in Table 1. The atomic factors for neutral atoms were taken from ref. 18 and values for the anomalous dispersion correction $\Delta f'$ and $\Delta f''$ from Cromer and Liberman.[19]. The full-matrix least-squares refinement was performed with a local modification of the SFLS-5 program.[20]

Full crystallographic details, excluding structure factors, have been deposited at the Cambridge Crystallographic Data Centre (CCDC). See Information for Authors, 1999, Issue 1. Any request to the CCDC for this material should quote the full literature citation and the reference number 1145/141.

Results and discussion

Single crystal data refinements led to the $Sr_{0.5}Bi_{0.96}$–, $Pb_{0.4}Bi_{1.2}$–, $K_{0.2}Bi_{1.45}$– and $Tl_{0.41}Bi_{1.24}$–V_8O_{16} stoichiometries while Feldmann and Müller–Buschbaum recently refined the $Ba_{0.5}Bi_{0.9}V_8O_{16}$ crystal structure.[15] It is instructive to note that the Sr, Pb and Tl compound stoichiometries are close to EDS analysis predictions while the much lighter K^+ cations were overvalued. Atomic coordinates and isotropic equivalent displacement parameters are given in Table 2. Because of the similar scattering factors for Tl^+, Pb^{2+} and Bi^{3+}, the latter was assigned to its crystallographic position with the help of its location in the $Bi_{1.62}V_8O_{16}$ framework. It turns out that Tl^+ is slightly displaced from the 2(b) (0,0,1/2) position for $Tl_{1.74}V_8O_{16}$ [7] to a 4(e) [0,0,z = 0.576(5)] crystallographic position for $Bi_{1.62}V_8O_{16}$.[11] By contrast, Pb^{2+} occupying the 4(f) [0,0,z = 0.230(1)] position of the monoclinic $Pb_{1.32}V_{8.35}O_{16.7}$, space group $I2/m$, is located in the 2(b) special position of $Bi_{1.2}Pb_{0.4}V_8O_{16}$. One could deduce a mean tunnel occupancy close to 1.6 using our single crystal growth method in good agreement with the $Bi_{1.62}V_8O_{16}$ single crystal results.[11] Furthermore, starting from a $ABiV_8O_{16}$ powder composition, hollandite-like tunnels accomodate preferentially Bi^{3+} cations while A^{n+} hosts appear weakly introduced in the obtained single crystals. In the selected crystals monoclinic distorted hollandite specimens were not encountered as, for instance in the vanadium-deficient solid solution $BaV_{10-x}O_{17}$.[21] In the latter, the tunnels accommodate an additional V atom which distorts the framework strongly.

Bi^{3+} environment

Selected interatomic distances are given in Table 3. The Bi^{3+} coordination does not drastically change from the $Bi_{1.62}V_8O_{16}$ results, in the sense that Bi^{3+} remains statistically displaced above and below the 2(a) (0,0,0) position leading to a practically square-planar coordination with four Bi–O(1) distances ranging from 2.443(5) Å in $Sr_{0.5}Bi_{0.96}V_8O_{16}$ to 2.514(8) Å in the $Tl_{0.41}Bi_{1.24}V_8O_{16}$ family member, Fig. 1(a). Bi^{3+} is a rather small cation and is naturally stabilized in this position which is approximately located at a distance from the nearest O(1) equal to the sum of the ionic radii. By contrast, in the average crystal structure of the incommensurate modulated $La_{1.16}Mo_8O_{16}$,[22] La^{3+} occupies the 2(b) (0,0,1/2) site despite its similar size and valence, r ($Bi^{3+\,(VIII)}$) = 1.17 Å and r ($La^{3+\,(VIII)}$) = 1.16 Å.[23] The z coordinate, Bi–$O(1)_4$ plane dis-

Table 2 Atomic coordinates and isotropic displacement parameters (Å^2) for $(A,Bi)_xV_8O_{16}$ phases (A = Sr, Pb, Ba, K, Tl)[a]

Atom	Site	Occupancy	x	y	z	B_{eq}/Å^2
$Bi_{1.7}V_8O_{16}$ [from ref. 11]						
Bi	4e	0.41(1)	0	0	0.1045(3)	1.62(3)
V	8h	1	0.3550(1)	0.1702(1)	0	0.54(2)
O	8h	1	0.1530(4)	0.1941(4)	0	0.59(6)
O	8h	1	0.5408(4)	0.1644(4)	0	0.64(6)
$Sr_{0.5}Bi_{0.96}V_8O_{16}$						
Bi	4e	0.24(1)	0	0	0.052(9)	2.0(3)
Sr	2b	0.26(1)	0	0	1/2	3.2(3)
V	8h	1	0.3541(1)	0.1704(1)	0	0.64(2)
O	8h	1	0.1527(5)	0.1927(5)	0	0.64(9)
O	8h	1	0.5401(5)	0.1652(5)	0	0.76(9)
$Pb_{0.4}Bi_{1.2}V_8O_{16}$						
Bi	4e	0.30(1)	0	0	0.113(4)	0.6(5)
Pb	2b	0.20(1)	0	0	1/2	6.0(7)
V	8h	1	0.3545(1)	0.1701(1)	0	0.52(4)
O	8h	1	0.1529(5)	0.1932(5)	0	0.6(2)
O	8h	1	0.5400(5)	0.1647(5)	0	0.5(2)
$Ba_{0.5}Bi_{0.9}V_8O_{16}$ [from ref. 15]						
Bi	4e	0.225(-)	0	0	0.0656(7)	2.45(8)
Ba	2b	0.25(-)	0	0	1/2	1.50(8)
V	8h	1	0.3535(1)	0.1697(1)	0	0.95(8)
O	8h	1	0.1538(3)	0.1954(3)	0	1.18(8)
O	8h	1	0.5406(3)	0.1648(3)	0	0.95(8)
$K_{0.2}Bi_{1.45}V_8O_{16}$						
Bi	4e	0.36(1)	0	0	0.0943(1)	1.59(2)
K	2b	0.10(1)	0	0	1/2	1.2(4)
V	8h	1	0.3547(1)	0.1700(1)	0	0.53(1)
O	8h	1	0.1534(3)	0.1945(3)	0	0.63(4)
O	8h	1	0.5405(3)	0.1644(3)	0	0.65(4)
$Tl_{0.41}Bi_{1.24}V_8O_{16}$						
Bi	4e	0.31(1)	0	0	0.093(1)	1.34(6)
Tl	4e	0.10(1)	0	0	0.576(5)	2.09(5)
V	8h	1	0.3544(2)	0.1698(2)	0	0.43(4)
O	8h	1	0.1551(7)	0.1963(8)	0	0.5(1)
O	8h	1	0.5396(7)	0.1647(7)	0	0.5(1)

B_{eq} is defined as $4/3\Sigma_i\Sigma_j\beta_{ij}a_ia_j$. U_{ij} is defined as $\exp[-2\pi^2(U_{11}h^2a^{*2}+...+2U_{23}klb^*c^*)]$.

tance and O(1)–Bi–O(1) angle are collected, and presented *vs.* the A^{n+} ionic radius in Table 4. In the case of consecutive Bi^{3+} cations along the tunnel cavities, the coordination is completed by the stereoactive $6s^2$ lone pair that should balance toward the empty side of the next $O(1)_4$ plane insuring a good electronic continuity along the *c* axis.

A^{n+} environment

It is observed that K^+, Sr^{2+} and Ba^{2+} are located in the 2(b) site yielding a regular square prismatic coordination, Fig. 1(b). Tl^+ and Pb^{2+} are both $6s^2$ lone pair cations, isoelectronic with Bi^{3+}. Attempts to delocalize Pb^{2+} at both sides of its final 2(b) site increased the reliability factors but its large

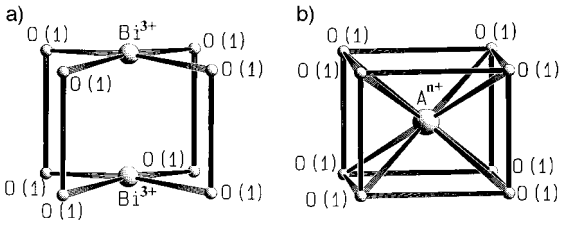

Fig. 1 Oxygen coordination polyhedra in $A^{n+}{}_xBi^{3+}{}_yV_8O_{16}$ (A = K,Sr, Ba, Pb) compounds around a: Bi^{3+}, b: A^{n+}.

associated *B* value of 6.0(7) Å^2 is still in favour of a stereoactive $6s^2$ lone pair effect. This phenomenon is clearly evidenced in the thallium compound, Tl^+ being statistically 0.22 Å at both sides of the 2(b) site. That leads to two Tl–O(1) distances, a short one of 2.784(9) Å and a longer one of 3.006(10) Å.

Generally, considering the hollandite tunnels formal occupancy that predicts the presence of *ca.* 20% vacancies, a statistic disorder between □, A^{n+} and Bi^{3+} is observable. □ vacancies would insure the transition between $-Bi^{3+}-Bi^{3+}-\cdots-Bi^{3+}-$ occupying tunnel portions and similar A^{n+} portions. No supercell spots were evident on oscillation and Weissenberg photographs of the studied crystals.

Powder investigation

$ABiV_8O_{16}$ phases. The phases were prepared as reported in the Experimental section. X-Ray powder diffraction patterns are shown in Fig. 2 and were indexed and least-squares refined in the tetragonal hollandite-like unit cell. Therefore, one should observe the presence of weak unidentified impurities for both $NaBiV_8O_{16}$ and $SrBiV_8O_{16}$. Our results on Pb/Bi hollandites highlighted a major difference compared to the work of Ramakrishnan *et al.*:[19] effectively, they were not able to obtain a single $Bi_{1.7-x}Pb_xV_8O_{16}$ material above $x = 0.4$. The unit-cell parameters are reported in Table 5 with their corresponding F_n criterion as defined by Smith and Snyder.[24] It shows the *a* parameter slightly increasing with the A^{n+} ionic radius while *c* remains almost constant. Considering the A^{n+} location in the 2(b) (0,0,1/2) site and the fully occupied character of the large tunnels in $ABiV_8O_{16}$ compounds, A^{n+} and Bi^{3+} cohabitation in the same tunnels is excluded as it would lead to unrealistic A^{n+}–Bi^{3+} distances of ≈1.45 Å. A intratunnel segregation is expected but does not appear ordered in the powder diffraction patterns. Therefore the larger section size of the A^{n+} filled tunnels play an active role towards the *a* parameters which range from 9.918(2) Å for $SrBiV_8O_{16}$ to 9.990(2) Å for $TlBiV_8O_{16}$. The Na^+ example appears to be an erratic point within this evolution. However, it is actually as expected given its location in the 2(a) (0,0,0) site that was evidenced in the oxide $Na_xMn_8O_{16}$.[25] Thus, Bi^{3+} and Na^+

Table 3 Interatomic distances (Å) for $(A,Bi)_xV_8O_{16}$ hollandite-type compounds

	$Bi_{1.7}V_8O_{16}$	$Sr_{0.5}Bi_{0.96}V_8O_{16}$	$Pb_{0.4}Bi_{1.2}V_8O_{16}$	$Ba_{0.5}Bi_{0.9}V_8O_{16}$	$K_{0.2}Bi_{1.45}V_8O_{16}$	$Tl_{0.41}Bi_{1.24}V_8O_{16}$
V octahedra						
V–O(1) (×1)	2.020(4)	2.010(5)	2.009(5)	2.002(3)	2.018(3)	2.009(7)
V–O(1) (×2)	1.986(2)	1.986(3)	1.980(3)	1.974(2)	1.982(2)	1.974(6)
V–O(2) (×1)	1.845(4)	1.845(5)	1.837(5)	1.850(3)	1.850(3)	1.851(7)
V–O(2) (×2)	1.953(2)	1.950(3)	1.944(3)	1.949(2)	1.949(2)	1.956(5)
Bi^{3+} Environment						
Bi–O(1) (×4)	2.473(2)	2.443(5)	2.461(5)	2.480(3)	2.480(3)	2.514(8)
A^{n+} Environment						
A–O(1) (×8)	—	2.836(4)	2.834(4)	2.865(3)	2.860(3)	4 × 2.784(9)
	—					4 × 3.006(10)
A–O(2) (×4)	—	3.344(5)	3.343(5)	3.358(3)	3.364(3)	3.380(7)

Table 4 Bismuth atom z coordinate, Bi to O(1) plane distance and O(1)–Bi–O(1) angle (°) for $(A,Bi)_xV_8O_{16}$ hollandite-type compounds

	$Bi_{1.7}V_8O_{16}$	$Sr_{0.5}Bi_{0.96}V_8O_{16}$	$Pb_{0.4}Bi_{1.2}V_8O_{16}$	$Ba_{0.5}Bi_{0.9}V_8O_{16}$	$K_{0.2}Bi_{1.45}V_8O_{16}$	$Tl_{0.41}Bi_{1.24}V_8O_{16}$
$r(A^{n+})$	—	1.26	1.29	1.42	1.51	1.59
z	0.104	0.051	0.112	0.065	0.09	0.093
Bi–plane/Å	0.30	0.144	0.324	0.188	0.261	0.270
Angle/°	166	173	164.8	171.2	167.3	167.7

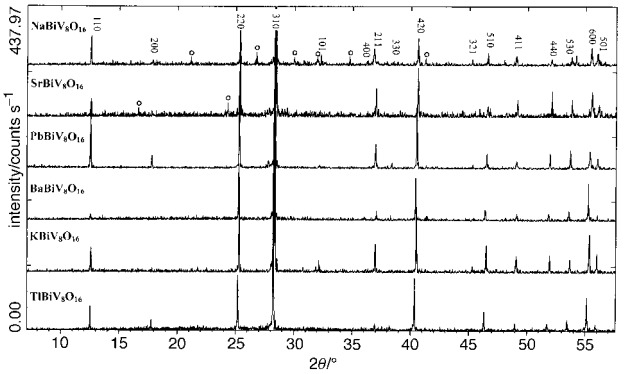

Fig. 2 Indexed X-ray powder diffraction pattern for mixed A/Bi vanadium hollandites; circles indicate impurity lines.

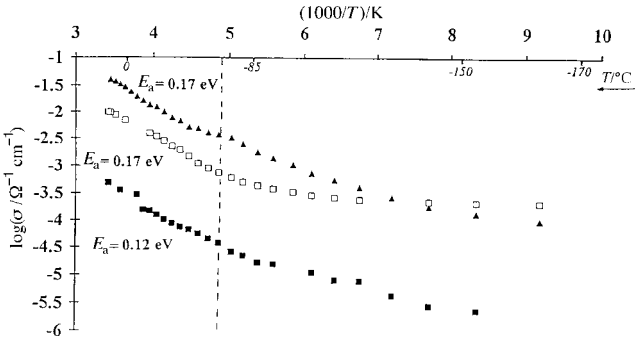

Fig. 3 Log σ *versus* $1000/T$ for $KBiV_8O_{16}$ (▲), $Bi_{1.62}V_8O_{16}$ (□) and $K_{0.8}Bi_{0.82}V_8O_{16}$ (■) phases.

can easily substitute for each other in the same tunnel in good agreement with their almost identical a parameters.

$K_xBi_yV_8O_{16}$ phases. Because previous work on potassium vanadium hollandite-like oxides reported that high pressure conditions were necessary to prepare $K_{1.8}V_8O_{16}$ and $K_2V_8O_{16}$ (3–7 GPa, 1200 °C[3]) while we introduced both K^+ and Bi^{3+} by a conventional vacuum solid state route, we thought it would be of interest to prepare intermediate compositions between $Bi_{1.62}V_8O_{16}$ and $K_{1.62}V_8O_{16}$. The global $x+y=1.62$ occupancy was chosen leading to the synthesis of $K_{1.62}V_8O_{16}$, $Bi_{1.4}K_{0.22}V_8O_{16}$, $Bi_{0.8}K_{0.82}V_8O_{16}$ and $Bi_{1.62}V_8O_{16}$. We also mention results concerning $KBiV_8O_{16}$. As expected, the potassium-only preparation did not lead to the formation of any hollandite-like compounds while for other compositions hollandite-phases were obtained pure. Least-squares refined unit cell parameters are given in Table 6. A slight increase of the a parameter is observed with increasing K^+ content reflecting the relatively large size of K^+ compared to Bi^{3+}, $r(K^+)/r(Bi^{3+})=1.51$ Å/1.17 Å. The c parameter is not influenced by the K/Bi ratio. The relative intensities of the 110, 200 and 220 reflections were measured using the 310 reflection as the $I=100$ standard, to confirm the effective reaction of K^+. Unreacted KVO_3 was not detected among bismuth rich phases, Table 5. The theoretical intensities were calculated from the crystallographic data using a local adaptation of the LAZY-PULVERIX[26] program. Observed and calculated relative intensities behave similarly. It can be concluded that the presence of Bi^{3+} aids the simultaneous introduction of K^+ in the V_8O_{16} framework. For $K/Bi>1$ compositions, pure powders are obtained.

Electric measurements. Conductivity measurements were performed down to liquid nitrogen temperature using a conventional four-probe cell. Log(σ) *vs.* $1000/T$ curves are presented in Fig. 3. They must be carefully examined since the polycrystalline samples response includes grain boundary contributions and contact resistivity which vary with the samples. Nevertheless a general 'two domains' behavior is observed up to *ca.* 70 °C which seems to be a transition temperature. The activation energy of the high-temperature fairly linear

Table 5 Unit cell parameters for $A^{n+}Bi^{3+}V_8O_{16}$ materials *vs.* the ionic radii of A

	$Bi_{1.7}V_8O_{16}$[a]	$NaBiV_8O_{16}$	$SrBiV_8O_{16}$	$PbBiV_8O_{16}$	$BaBiV_8O_{16}$	$KBiV_8O_{16}$	$TlBiV_8O_{16}$
$r(A^{n+})$	1.17	1.18	1.26	1.29	1.42	1.51	1.59
a /Å	9.930(4)	9.934(5)	9.918(2)	9.938(2)	9.956(2)	9.952(1)	9.990(2)
c/Å	2.914(1)	2.913(2)	2.895(1)	2.897(1)	2.887(1)	2.901(1)	2.897(1)
F	$F_{19}=75.3$ (0.009,28)	$F_{18}=39.1$ (0.023,20)	$F_{14}=87.5$ (0.008,20)	$F_{15}=88.3$ (0.01,17)	$F_{15}=150$ (0.005,20)	$F_{14}=116.6$ (0.006,20)	$F_{14}=66.7$ (0.01,20)

[a]From ref. 11.

Table 6 Calculated intensity *vs.* measured intensity for (110), (200), (220) and (310) reflections for $(A,Bi)_xV_8O_{16}$ materials

	a and c parameters/Å	110 I_{theo}/I_{meas}	200 I_{theo}/I_{meas}	220 I_{theo}/I_{meas}	310 I_{theo}/I_{meas}
$Bi_{1.62}V_8O_{16}$	$a=9.331(7)$, $c=2.9116(4)$	26.7/26.7	5.7/7.7	30.1/49.2	100/100
$Bi_{1.4}K_{0.22}V_8O_{16}$	$a=936(1)$, $c=2.9104(5)$	15.1/12.1	2.0/4.2	27.2/29.3	100/100
$Bi_{0.8}K_{0.82}V_8O_{16}$	$a=9.957(2)$, $c=2.9016(9)$	0.5/3.8	1.1/—	20.6/20.4	100/100
$BiKV_8O_{16}$	$a=9.963(5)$, $c=2.916(2)$	6.5/4.7	0.1/—	24.3/21.7	100/100

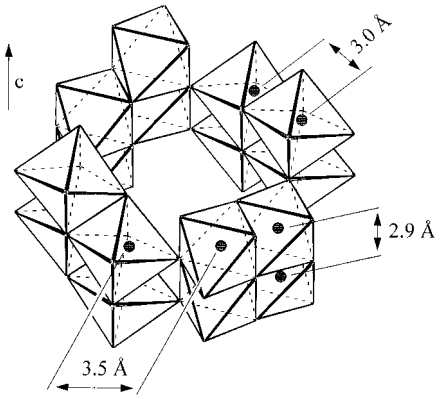

Fig. 4 Hollandite tunnels section and V–V distances.

Arrhenius plot is close to 0.15 eV and probably indicates hopping semi-conduction. Tunnel walls are formed by double rutile chain sharing corners to form 2×2 octahedral tunnels. V–V distances within one rutile chain are close to 2.9 Å and V–V distances between vanadium ions of a double chain are close to 3.0 Å. The V–V distances between two different walls is 3.5 Å indicating the absence of d–d overlapping, Fig. 4. Electronic transfer is expected to occur in a direction parallel to *c*. Thus, depending on the predominant V^{3+}/V^{4+} species, electronic motion is expected to arise from the transfer of extra holes or electrons to the acceptors of the same tunnel wall. $KBiV_8O_{16}$ exhibits a V^{3+}/V^{4+} ratio of unity and would be an interesting example for a full electric/magnetic investigation.

References

1 F. Gronvold, H. Haraldsen, B. Pedersen and T. Tufte, *Rev. Chim. Miner*., 1969, **6**, 215.
2 F. Cansell, *Presented at the Galerne 98 Summer school*, La Rochette, Oct. 1998.
3 J. B. Sokoloff, *Phys. Rev. B*, 1978, **17**, 4843.
4 S. K. Khanna, G. Grüner, R. Orbach and H. U. Beyeler, *Phys. Rev. Lett*., 1981, **47**, 255.
5 A. E. Ringwood, S. E. Kesson, N.G. Ware, W. Hibberson and A. Major, *Nature*, 1979, **278**, 219.
6 H. Okada, N. Kinomura and S. Kume, *Mater. Res. Bull*., 1978, **13**, 1047.
7 W. Abriel, F. Rau and K-J. Range, *Mater. Res. Bull*., 1979, **14**, 1463.
8 W. Abriel, C. Garbe, F. Rau and K-J. Range, *Z. Kristallogr*., 1986, **176**, 113.
9 W. Abriel and K-J Range, *Z. Kristallogr*., 1987, **178**, 225.
10 Y. Kanke, E. Takayama-Muromachi, K. Kato and K. Kosuda, *J. Solid State Chem*., 1995, **115**, 88.
11 F. Abraham and O. Mentre, *J. Solid State Chem*., 1994, **109**, 127.
12 A. Byström and A. M. Byström, *Acta Crystallogr*., 1950, **3**, 146.
13 O. Mentre and F. Abraham, *J. Solid State Chem*., 1996, **125**, 91.
14 J. Feldmann and Hk. Müller–Buschbaum, *Z. Naturforsch.*, *Teil B*, 1995, **50**, 1163.
15 J. Feldmann and Hk. Müller–Buschbaum, *Z. Naturforsch.*, *Teil B*, 1996, **51**, 1037.
16 P. A. Ramakrishnan, M. Sugantha, U. V. Vadaraju and T. Nagarajan, *Mater. Lett.*., 1998, **36**, 137.
17 J. De Meulenaer and H. Tompa, *Acta Crystallogr*., 1965, **19**, 1014.
18 *International Tables for X-Ray Crystallography*, Kynoch Press, Birmingham, 1974, vol. 4.
19 D. T. Cromer and D. Liberman, *J. Chem. Phys*., 1970, **53**, 1891.
20 C. T. Prewitt, SFLS-5, Report ORNL- TM 305 Oak Ridge National Laboratory, Oak Ridge, Tennessee, 1966.
21 Y. Kanke, E. Takayama-Muromachi, K. Kato and K. Kosuda, *J. Solid State Chem*., 1994, **113**, 125.
22 H. Leligny, Ph. Labbe, M. Ledesert and B. Raveau, *Acta Crystallogr.*, *Sect. B*, 1992, **48**, 134.
23 R. D. Shannon, *Acta Crystallogr*., *Sect. A*, 1976, **32**, 751.
24 G. Smith and R. L. Snyder, *J. Appl. Cryst*., 1979, **12**, 60.
25 R. Giovanoli and M. Faller, *Chimia*, 1989, **43**, 54.
26 K. Yvon, W. Jeitschko and E. Parthe, *J. Appl Crystallogr*., 1977, **10**, 73.

Paper 8/09552C